Med Chem Res
DOI 10.1007/s00044-017-2003-x

MEDICINAL CHEMISTRY RESEARCH

ORIGINAL RESEARCH

Synthesis and neuroprotective activity of novel 1,2,4-triazine derivatives with ethyl acetate moiety against H_2O_2 and Aβ-induced neurotoxicity

Tuba Tuylu Kucukkilinc[1] · Kamaledin Safari Yanghagh[2] · Beyza Ayazgok[1] · Mohammad Ali Roknipour[2] · Farshad Homayouni Moghadam[3] · Alireza Moradi[4] · Saeed Emami[5] · Mohsen Amini[6] · Hamid Irannejad[5]

Received: 21 March 2017 / Accepted: 25 July 2017

Abstract A series of 5,6-diaryl-1,2,4-triazine-3-thioacetate derivatives **3a–f**, **8a–d** and their regioisomer **8e** were synthesized. Neuroprotective activity of compounds was assessed against H_2O_2 and β-amyloid-induced toxicity in PC12 and SH-SY5Y cells respectively. Surprisingly, ethyl 2-(5-(4-chlorophenyl)-6-(4-methoxyphenyl)-3-thioxo-1,2,4-triazin-2(3H)-yl)acetate (**8e**) was the most potent compound in both tests with EC_{50} of 14 μM in H_2O_2 induced apoptosis and also could increase 40% of cell viability revealed by cytometric analysis with Annexin V/PI staining. It was also shown that regioisomer **8e** has more neuroprotective activity than Quercetin in β-amyloid induced toxicity. Morphologic evaluation of cells by DAPI staining and TUNEL assay showed the effectiveness of this compound to improve neurite outgrowth in neuronal cells.

Keywords Synthesis · 1,2,4-triazine · Alzheimer's disease · Apoptosis · Neuroprotective activity

Introduction

Alzheimer's disease (AD) is a complex pathologic disorder characterized by intracellular neurofibrillary tangles and extracellular amyloid aggregates in the CNS tend to neurodegeneration, impairment to memory and cognitive deficits (Butterfield 2002). Pathological deterioration in AD is substantially associated to the overproduction of β-amyloid (Aβ) peptide that is generated by the successive action of β and γ-secretases on the amyloid precursor protein (APP) (Nunan and Small 2000). Two variants of β-amyloids are normally found in the brain of AD patients: Aβ (1–40) and Aβ (1–42), in which β-amyloid (1–42) is the most dominant and toxic form of β-amyloid in AD (Findeis 2007). β-amyloid peptides are highly prone to self-aggregation and form fibrillar plaques in neuronal cells. Accordingly, β-amyloid aggregates in AD has been associated with overproduction of reactive oxygen species (ROS) and radicals which damage cellular and biological macromolecules like DNA and protein oxidation that usually leads to acute inflammation, necrosis and eventually apoptosis (Heneka et al. 2010; Pimplikar 2009).

In recent years, numerous approaches have been used to combat AD through different mechanisms like small molecule inhibitors of β-amyloid aggregation (Geng et al. 2011), anti-inflammatory agents (Cheng et al. 2015), inhibitors of cyclooxygenase (Manev et al. 2011),

Electronic supplementary material The online version of this article (doi:10.1007/s00044-017-2003-x) contains supplementary material, which is available to authorized users.

✉ Hamid Irannejad
irannejadhamid@gmail.com

[1] Department of Biochemistry, Faculty of Pharmacy, Hacettepe University, Sihhiye, 06100 Ankara, Turkey

[2] Student Research Committee, Faculty of Pharmacy, Mazandaran University of Medical Sciences, Sari, Iran

[3] Department of Cellular Biotechnology at Cell Science Research Center, Royan Institute for Biotechnology, ACECR, Isfahan, Iran

[4] Department of Medicinal Chemistry, Faculty of Pharmacy and Pharmaceutical Sciences Research Center, Shahid Sadoughi Yazd University of Medical Sciences, Yazd, Iran

[5] Department of Medicinal Chemistry, Pharmaceutical Sciences Research Center, Faculty of Pharmacy, Mazandaran University of Medical Sciences, Sari, Iran

[6] Department of Medicinal Chemistry, Drug Design & Development Research Center, Faculty of Pharmacy, Tehran University of Medical Sciences, Tehran, Iran

Published online: 04 August 2017

cholinesterase (Raina et al. 2008), β-secretase, and γ-secretase (Ghosh and Osswald 2014).

Triazine-based compounds have been an interesting scaffold for design and development of anti-Alzheimer's drugs. Previously, some s-triazine derivatives were synthesized and evaluated as inhibitors of acetylcholinesterase (AChE) and β-amyloid aggregates (Veloso et al. 2013). Moreover, triazine derivatives have been found to attenuate the ROS production, caspase-3 activation and the extent of apoptotic cell death induced by β-amyloid (1–42) (Shaykhalishahi et al. 2010).

Particularly, investigation on 5,6-diaryl-1,2,4-triazine derivatives against H_2O_2-induced apoptosis in a neuronal cell line showed the ability of these compounds to inhibit oxidative stress-mediated phosphorylation of MAP kinases and improvement of cells neurite outgrowth (Khodagholi et al. 2012a, b). Further studies by our research group on the protective effect of the same analogs (Fig. 1a) against H_2O_2-induced apoptosis in PC12 cells showed the increasing level of stress sensing transcription factor, NF-E2 related factor 2 and NF-κB which both contribute to cell survival. We have also showed that 5,6-diaryl-1,2,4-triazine compounds are able to suppress the expression of cyclooxygenase-2 which is one of the inflammatory key enzymes involved in AD progression (Ansari et al. 2010; Irannejad et al. 2010). It was also shown that elevated levels of glutathione peroxidase-1, glutamylcysteine synthetase, and glutathione, as well as superoxide dismutase and catalase affected by 5,6-diaryl-1,2,4-triazine derivatives, increased antioxidant capacity of cells (Khodagholi et al. 2012a, b; Khoramian Tusi et al. 2010). Some 3-substituted-5,6-diphenyl-1,2,4-triazine derivatives (Fig. 1b) have been also introduced as neuroprotective agents through inhibition of cholinesterase enzyme (Sinha et al. 2015).

Recently, we synthesized 1,2,4-triazine-3-thioacetate derivatives (Fig. 1c) and evaluated their COX-2 inhibitory activity and β-amyloid disaggregation ability (Dadashpour et al. 2015). The obtained results indicated that these compounds act as highly β-amyloid destabilizing agents, dissolving 80–95% of β-amyloid aggregates in 24 h. Herein, we report synthesis of some symmetrical and unsymmetrical 5,6-diaryl-1,2,4-triazines **3a–f** and **8a–e** (Fig. 2) as potential agents for treatment of AD. We evaluated them against both H_2O_2 and β-amyloid induced toxicity in PC-12 (pheochromocytoma of the rat adrenal medulla) and SH-SY5Y (human neuroblastoma) cells and the extent of cell viability and apoptosis were assessed during 24 and 48 h of treatment.

Material & methods

Chemistry

All commercially available reagents were purchased from Merck or Aldrich and used without further purification. Column chromatography was carried out on silica gel (230–400 mesh). Thin layer chromatography (TLC) was conducted on silica gel F254 plates. Infrared (IR) spectra were taken using Perkin-Elmer Fourier transform infrared (FT-IR) (KBr disks). Mass spectra were obtained on an Agilent 5937 Mass Selective Detector. Nuclear magnetic resonance (NMR) spectra were recorded on a Bruker 400 or 500 MHz instruments. The chemical shifts (δ) and coupling constants (J) are expressed in ppm and Hertz (Hz), respectively. Elemental analyzes were carried out by ECS-4010 (Costech International S.p.A.) elemental analyzer. The

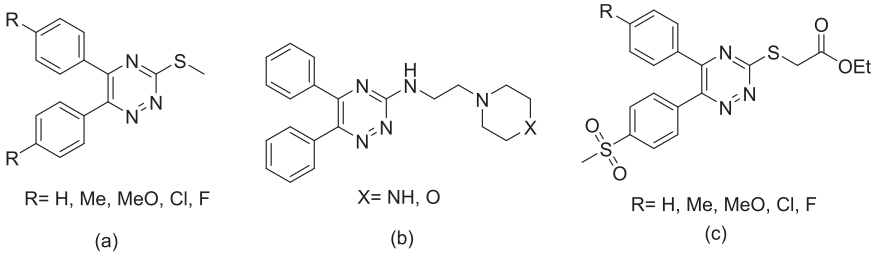

Fig. 1 Structures of previously reported compounds as **a** potent neuroprotective agents against LPS and H_2O_2-induced toxicity on PC12 cells. **b** Neuroprotective agents through cholinesterase inhibition. **c** COX-2 and β-amyloid aggregation inhibitors

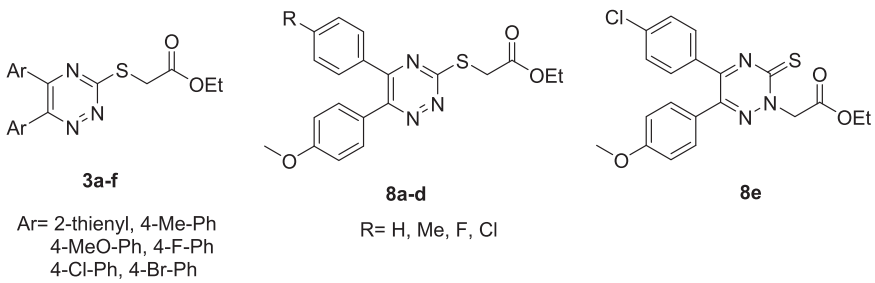

Fig. 2 Structures of newly synthesized compounds as neuroprotective agents against H_2O_2 and β-amyloid induced toxicity

results of elemental analyzes (C, H, N) were within ±0.4% of the calculated values.

General procedure for the synthesis of compounds ***2a–f***

To a stirred solution of appropriate 1,2-diketone **1a–f** (1 mmol) and thiosemicarbazide (1.1 mmol) in a mixture of water and ethanol (1:1), was added a few drops of concentrated hydrochloric acid and resulting mixture was irradiated under microwave at 130 °C for 20 min. After cooling to room temperature, it was filtered and washed with water to give the desired product. This procedure in detail along with structural characterization data of compounds has been reported in our recently published study (Irannejad et al. 2014, 2015).

General procedure for the synthesis of compounds ***3a–f***

To a stirred solution of 5,6-diaryl-1,2,4-triazine-3-thiol derivatives **2a–f** (1 mmol) in DMSO (25 ml) was added ethyl chloroacetate (1.5 mmol) and K_2CO_3 (2 mmol) and it was stirred for 10 h under nitrogen atmosphere. After completion of the reaction, it was diluted by ethyl acetate and washed with water three times. The organic phase was dried over sodium sulfate and concentrated under vacuum. Purification was performed by column chromatography. Silica gel was used as stationary phase and eluent was 10–20% of ethyl acetate in petroleum ether.

Ethyl 2-((5,6-di(thiophen-2-yl)-1,2,4-triazin-3-yl)thio)acetate (**3a**) Yield 86%, IR (KBr, cm^{-1}) υ_{max}: 1743 (C=O). ^{1}H NMR (400 MHz, $CDCl_3$) δ (ppm): 1.3 (t, $J = 7.12$ Hz, 3H, $CH_2\underline{CH_3}$), 4.08 (s, 2H, SCH_2CO), 4.26 (q, $J = 7.12$ Hz, 2H, $\underline{CH_2}CH_3$), 7.02 (dd, $J = 5$ and 3.9 Hz, 1H), 7.14 (dd, $J = 5$ and 3.6 Hz, 1H), 7.40 (dd, $J = 3.6$ and 1.1 Hz, 1H), 7.46 (dd, $J = 3.9$ and 1.0 Hz, 1H), 7.57 (dd, $J = 5$ and 1.1 Hz, 1H), 7.59 (dd, $J = 5$ and 1 Hz, 1H). ^{13}C NMR (100 MHz, $CDCl_3$) δ (ppm): 14.19, 33.15, 62.02, 127.69, 128.45, 129.11, 129.27, 132.51, 133.20, 136.38, 138.63, 147.07, 149.08, 168.54, 168.91. MS, *m/z* (%): 363.0 (M^+, 25), 317.9 (9), 263.9 (7), 189.9 (100), 157.9 (12), 144.9 (23), 110.9 (44). Anal. calcd. for $C_{15}H_{13}N_3O_2S_3$: C, 49.57; H, 3.61; N, 11.56. Found: C, 49.61; H, 3.72; N, 11.69.

Ethyl 2-((5,6-di-p-tolyl-1,2,4-triazin-3-yl)thio)acetate (**3b**) Yield 80%, IR (KBr, cm^{-1}) υ_{max}: 1735 (C=O). ^{1}H NMR (400 MHz, $CDCl_3$) δ (ppm): 1.25 (t, $J = 7.9$ Hz, 3H, $CH_2\underline{CH_3}$), 2.38 (s, 3H, Ar–CH_3), 2.39 (s, 3H, Ar–CH_3), 4.11 (s, 3H, SCH_2CO), 4.24 (q, $J = 7.16$ Hz, 2H, $\underline{CH_2}CH_3$), 7.14 (d, $J = 7.96$ Hz, 2H, Ar–H), 7.18 (d, $J = 7.88$ Hz, 2H, Ar–H), 7.42 (d, $J = 7.96$ Hz, 2H, Ar–H), 7.47 (d, $J = 8.08$ Hz, 2H, Ar–H). ^{13}C NMR (100 MHz, $CDCl_3$) δ (ppm): 14.15, 21.40, 21.51, 33.19, 61.91, 129.20, 129.34, 129.84, 130.02, 132.25, 132.45, 139.56, 141.56, 154.07, 155.42, 168.77, 168.81. MS, *m/z* (%): 379.1 (M^+, 38), 334.0 (24), 238.0 (27), 206.0 (100), 189.0 (34), 119.0 (83). Anal. calcd. for $C_{21}H_{21}N_3O_2S$: C, 66.47; H, 5.58; N, 11.07. Found: C, 66.51; H, 5.62; N, 11.09.

Ethyl 2-((5,6-bis(4-methoxyphenyl)-1,2,4-triazin-3-yl)thio) acetate (**3c**) Yield 75 %; IR (KBr, cm^{-1}) υ_{max}: 1730 (C=O). ^{1}H-NMR (400 MHz, $CDCl_3$) δ (ppm): 1.28 (t, $J = 7.2$ Hz, 3H, $CH_2\underline{CH_3}$), 3.83 (s, 3H, OCH_3), 3.85 (s, 3H, OCH_3), 4.1 (s, 2H, SCH_2CO), 4.23 (q, $J = 7.2$ Hz, 2H, $\underline{CH_2}CH_3$), 6.84 (d, $J = 8.9$ Hz, 2H, Ar–H), 6.91 (d, $J = 8.9$ Hz, 2H, Ar–H), 7.48 (d, $J = 8.9$ Hz, 2H, Ar–H), 7.56 (d, $J = 8.9$ Hz, 2H, Ar–H). ^{13}C-NMR (100 MHz, $CDCl_3$) δ (ppm): 14.15, 33.17, 55.32, 55.38, 61.87, 113.93, 114.13, 127.26, 127.84, 130.63, 131.66, 153.50, 154.71, 160.61, 161.98, 168.32, 168.84. MS, *m/z* (%): 411.1 (M^+, 29), 280.9 (34), 238.0 (53), 206.9 (56), 191.0 (33), 162.9 (39), 135 (100). Anal. calcd. for $C_{21}H_{21}N_3O_4S$: C, 61.30; H, 5.14; N, 10.21. Found: C, 61.41; H, 5.23; N, 10.29.

Ethyl 2-((5,6-bis(4-fluorophenyl)-1,2,4-triazin-3-yl)thio)acetate (**3d**) Yield 51 %, IR (KBr, cm^{-1}) υ_{max}: 1734 (C=O), 1602 (C=N). ^{1}H NMR (400 MHz, $CDCl_3$) δ (ppm): 1.34 (t, $J = 7.12$ Hz, 3H, $CH_2\underline{CH_3}$), 4.11 (s, 2H, SCH_2CO), 4.24 (q, $J = 7.2$ Hz, 2H, $\underline{CH_2}CH_3$), 7.07 (t, $J = 8.5$ Hz, 2H, Ar), 7.14 (t, $J = 8.6$ Hz, 2H, Ar), 7.50 (dd, $J = 8.8$ and 5.28 Hz, 2H, Ar), 7.56 (dd, $J = 8.8$ and 5.28 Hz, 2H, Ar). ^{13}C-NMR (125 MHz, $CDCl_3$) δ (ppm): 14.11, 33.17, 61.25, 115.84 (d, $J = 10.0$ Hz), 116.02 (d, $J = 10.0$ Hz), 131.27 (d, $J = 8.8$ Hz), 132.09 (d, $J = 8.8$ Hz), 132.6 (d, $J = 10.0$ Hz), 153.02, 154.26, 163.6 (d, $J = 250.0$ Hz), 164.5 (d, $J = 252.5$ Hz), 168.56, 169.43. MS, *m*/z (%): 387.0 (M^+, 22), 342.0 (19), 214.0 (100), 192.9 (28), 122.9 (46). Anal. calcd. for $C_{19}H_{15}F_2N_3O_2S$: C, 58.91; H, 3.90; N, 10.85. Found: C, 59.06; H, 3.98; N, 10.89.

Ethyl 2-((5,6-bis(4-chlorophenyl)-1,2,4-triazin-3-yl)thio)acetate (**3e**) Yield 69%, IR (KBr, cm^{-1}) υ_{max}: 1734 (C=O), 1306 (C=N). ^{1}H NMR (400 MHz, $CDCl_3$) δ (ppm): 1.29 (t, $J = 7.16$ Hz, 3H, $CH_2\underline{CH_3}$), 4.11 (s, 2H, SCH_2CO), 4.24 (q, $J = 7.12$ Hz, 2H, $\underline{CH_2}CH_3$), 7.35 (d, $J = 8.6$ Hz, 2H, Ar–H), 7.38 (d, $J = 8.64$ Hz, 2H, Ar–H), 7.47 (d, $J = 8.6$ Hz, 2H, Ar–H), 7.5 (d, $J = 8.6$ Hz, 2H, Ar–H). ^{13}C-NMR (125 MHz, $CDCl_3$) δ (ppm): 14.12, 33.17, 61.96, 129.03, 129.13, 130.60, 131.13, 133.16, 133.36, 136.11, 137.76, 152.88, 154.17, 168.48, 169.66. MS, *m/z* (%): 421.0 (M^++2, 19), 419.0 (M^+, 27), 359.9 (24), 316.1 (33), 247.9 (68), 245.9 (100), 137.0 (43), 135.0 (74). Anal. calcd. for $C_{19}H_{15}Cl_2N_3O_2S$: C, 54.30; H, 3.60; N, 10.00. Found: C, 54.46; H, 3.78; N, 10.12.

Ethyl 2-((5,6-bis(4-bromophenyl)-1,2,4-triazin-3-yl)thio) acetate (**3f**) Yield 76%, IR (KBr, cm^{-1}) υ_{max}: 1724 (C=O). ^{1}H NMR (400 MHz, $CDCl_3$) δ (ppm): 1.29 (t, J = 7.16 Hz, 3H, $CH_2\underline{CH_3}$), 4.11 (s, 2H, SCH_2CO), 4.26 (q, J = 7.12, 2H, $\underline{CH_2}CH_3$), 7.40 (d, J = 8.8 Hz, 2H, Ar–H), 7.42 (d, J = 8.8 Hz, 2H, Ar–H), 7.52 (d, J = 8.8 Hz, 2H, Ar–H), 7.54 (d, J = 8.5 Hz, 2H, Ar–H). ^{13}C NMR (100 MHz, $CDCl_3$) δ (ppm): 14.16, 33.21, 62.05, 124.45, 126.27, 130.84, 131.31, 132.02, 132.11, 133.54, 133.72, 152.89, 154.31, 168.57, 169.69.MS, *m/z* (%): 509.8 (M^++2, 15), 462.9 (22), 413.9 (18), 335.8 (48), 316.3 (32), 238.0 (23), 159.9 (54). Anal. calcd. for $C_{19}H_{15}Br_2N_3O_2S$: C, 44.82; H, 2.97; N, 8.25. Found: C, 44.86; H, 3.08; N, 8.29.

*General procedure for the preparation of compounds **5a–d***

To a stirred solution of phenylacetic acid derivative (1 mmol), anisole (1.2 mmol) and phosphoric acid (1.2 mmol) was added trifluoroacetic acid anhydride (4 mmol) and stirred for 5 min at room temperature. Then crushed ice was added to the reaction mixture while stirring and the precipitate was filtered and washed with water and then petroleum ether respectively. The crude product was used in the next step without further purification.

*General procedure for the preparation of compounds **6a–d***

To a stirred solution of 1-(4-methoxyphenyl)-2-arylethanone **5a–d** (1 mmol) in methanol was added a prepared solution of sodium (1.5 mmol) in methanol and the resulting mixture was stirred for 5 min. Then butyl nitrite (1 mmol) was added and stirring was continued for 30 min. Reaction mixture was monitored by TLC. After completion of the reaction, it was concentrated under vacuum, diluted with water and pH was adjusted to neutral by adding HCl 10%. Aqueous phase was extracted three times with ethyl acetate, dried and evaporated. The residue was recrystalized from methanol to give pure compounds **6a–d**.

2-(Hydroxyimino)-1-(4-methoxyphenyl)-2-phenylethanone (**6a**) Yield 67%; mp: 107–109 °C; IR (KBr, cm^{-1}) υ_{max}: 1638 (C=O). ^{1}H-NMR (400 MHz, DMSO-d_6) δ (ppm): 3.84 (s, 3H, OCH_3), 7.11 (d, J = 9 Hz, 2H, Ar–H), 7.40–7.49 (m, 5H, Ar–H), 7.81 (d, J = 8.92 Hz, 2H, Ar–H), 11.69 (s, 1H, NOH).

2-(Hydroxyimino)-1-(4-methoxyphenyl)-2-p-tolylethanone (**6b**) Yield 54%; mp: 110–111 °C; IR (KBr, cm^{-1}) υ_{max}: 1667 (C=O). ^{1}H-NMR (400 MHz, DMSO-d_6) δ (ppm): 2.29 (s, 3H, Ar–CH_3), 3.84 (s, 3H, OCH_3), 7.09 (d, J = 8.88 Hz, 2H, Ar–H), 7.21 (d, J = 8.12 Hz, 2H, Ar–H), 7.36 (d, J = 8.2 Hz, 2H, Ar–H), 7.8 (d, J = 8.84 Hz, 2H, Ar–H), 11.57 (s, 1H, NOH). ^{13}C-NMR (100 MHz, DMSO-d_6) δ (ppm): 21.33, 56.16, 115.09, 125.98, 128.08, 129.57, 130.03, 131.78, 140.07, 155.23, 164.64, 193.89.

2-(4-Fluorophenyl)-2-(hydroxyimino)-1-(4-methoxyphenyl)ethanone (**6c**) Yield 65%; mp: 125–127 °C; IR (KBr, cm^{-1}) υ_{max}: 1643 (C=O). ^{1}H-NMR (400 MHz, DMSO-d_6) δ (ppm): 3.85 (s, 3H, OCH_3), 7.1 (d, J = 8.96 Hz, 2H, Ar–H),7.26 (t, J = 8.92 Hz, 2H, Ar–H), 7.51 (dd, J = 8.98 and 5.4 Hz, 2H, Ar–H), 7.81 (d, J = 8.92 Hz, 2H, Ar–H), 11.71 (s, 1H, NOH). ^{13}C-NMR (100 MHz, DMSO-d_6) δ (ppm): 56.19, 115.17, 116.60 (d, J = 21.91 Hz), 127.89, 128.33 (d, J = 8.46 Hz), 131.88, 132.19 (d, J = 8.54 Hz), 154.27, 161.23 (d, J = 251.1 Hz), 164.79, 193.56.

2-(4-Chlorophenyl)-2-(hydroxyimino)-1-(4-methoxyphenyl)ethanone (**6d**) Yield 52%; mp: 120 °C; IR (KBr, cm^{-1}) υ_{max}: 1669 (C=O). ^{1}H-NMR (400 MHz, DMSO-d_6) δ (ppm): 3.84 (s, 3H, OCH_3), 7.07 (d, J = 8.96 Hz, 2H, Ar–H),7.10 (d, J = 9.0 Hz, 2H, Ar–H), 7.82 (d, J = 8. 92 Hz, 2H, Ar–H), 7.96 (d, J = 8.96 Hz, 2H, Ar–H), 11.7 (s, 1H, NOH). ^{13}C-NMR (100 MHz, DMSO-d_6) δ (ppm): 56.18, 114.24, 115.16, 116.70, 127.90, 128.37, 131.88, 133.11. 154.28, 164.78, 193.57.

*General procedure for the preparation of compounds **7a–d***

To a stirred solution of 2-hydroxyimino-1-(4-methoxyphenyl)-2-arylethanone **6a–d** (1 mmol) in a mixture of water and ethanol (2:1), was added thiosemicarbazide (1.5 mmol) and five drops of conc. HCl and the resulting mixture was refluxed for 4 h. After cooling of reaction mixture, precipitate was filtered and washed with water. Crystallization was performed in ethanol.

*General procedure for the preparation of compounds **8a–e***

To a stirred solution of 6-(4-methoxyphenyl)-5-aryl-1,2,4-triazine-3-thiol **7a–d** (1 mmol) in DMSO (25 ml) was added ethyl chloroacetate (1.5 mmol) and K_2CO_3 (2 mmol) and it was stirred for 10 h under nitrogen atmosphere. After completion of reaction, it was diluted by ethyl acetate and washed by water three times. The organic phase was dried over sodium sulfate and concentrated under vacuum. Purification was performed by column chromatography. Silica gel (230–400 mesh) was used as stationary phase and eluent was 5% of ethyl acetate in chloroform. In this manner, compounds **8a–d** were isolated as major products.

Ethyl 2-(6-(4-methoxyphenyl)-5-phenyl-1,2,4-triazine-3-ylthio)acetate (**8a**) Yield 61%; IR (KBr, cm^{-1}) υ_{max}: 1741 (C=O). ^{1}H-NMR (400 MHz, $CDCl_3$) δ (ppm): 1.29 (t, J =

7.12 Hz, 3H, $CH_2\underline{CH_3}$), 3.83 (s, 3H, OCH_3), 4.11 (s, 2H, SCH_2CO), 4.22 (q, $J = 7.12$ Hz, 2H, $\underline{CH_2}CH_3$), 6.83 (d, $J = 8.92$ Hz, 2H, Ar–H), 7.39–7.43 (m, 3H, Ar–H), 7.53–7.56 (m, $J = 9.0$ Hz, 4H, Ar–H). ^{13}C-NMR (100 MHz, $CDCl_3$) δ (ppm): 14.15, 33.19, 55.39, 61.91, 113.93, 126.91, 128.68, 129.21, 129.39, 131.83, 135.70, 153.85, 154.92, 162.10, 168.81, 168.91. MS, *m/z* (%): 381.1 (M^+, 32), 327.0 (39), 299.0 (33), 252.9 (34), 226.9 (48), 208.0 (100), 135.0 (84). Anal. calcd. for $C_{20}H_{19}N_3O_3S$: C, 62.98; H, 5.02; N, 11.02. Found: C, 63.06; H, 5.09; N, 11.11.

Ethyl 2-(6-(4-(methoxyphenyl)-5-p-tolyl-1,2,4-triazine-3-ylthio)acetate (**8b**) Yield 60%; IR (KBr, cm^{-1}) υ_{max}: 1756 (C=O). ^{1}H-NMR (400 MHz, $CDCl_3$) δ (ppm): 1.09 (t, $J =$ 7.2 Hz, 3H, $CH_2\underline{CH_3}$), 2.32 (s, 3H, Ar–CH_3), 3.82 (s, 3H, OCH_3), 3.86 (s, 2H, SCH_2CO), 4.22 (q, $J = 7.16$ Hz, 2H, $\underline{CH_2}CH_3$), 6.92 (d, $J = 9.0$ Hz, 2H, Ar–H), 7.11 (d, $J = 8.0$ Hz, 2H, Ar–H), 7.41 (d, $J = 8.2$ Hz, 2H, Ar–H), 7.89 (d, $J = 9.0$ Hz, 2H, Ar–H). ^{13}C-NMR (125 MHz, $CDCl_3$) δ (ppm): 14.19, 21.26, 32.52, 55.28, 61.33, 114.06, 126.11, 126.55, 129.16, 129.41, 129.61, 139.71, 154.92, 159.43, 161.89, 169.63, 171.43. MS, *m/z* (%): 395.1 (M^+, 13), 339.2 (12), 281.0 (19), 255.7 (38), 207.0 (34), 191.1 (100). Anal. calcd. for $C_{21}H_{21}N_3O_3S$: C, 63.78; H, 5.35; N, 10.63. Found: C, 63.85; H, 5.39; N, 10.71.

Ethyl 2-(5-(4-fluorophenyl)-6-(4-methoxyphenyl)-1,2,4-triazine-3-ylthio) acetate (**8c**) Yield 53%; IR (KBr, cm^{-1}) υ_{max}: 1731 (C=O). ^{1}H-NMR (400 MHz, $CDCl_3$) δ (ppm): 1.11 (t, $J = 7.16$ Hz, 3H, $CH_2\underline{CH_3}$), 3.83 (s, 3H, OCH_3), 3.87 (s, 2H, SCH_2CO), 4.22 (q, $J = 7.16$ Hz, 2H, $\underline{CH_2}CH_3$), 6.93 (d, $J = 8.96$ Hz, 2H, Ar–H), 7.0 (t, $J = 8.72$ Hz, 2H, Ar–H), 7.5 (dd, $J = 8.84$ and 5.44 Hz, 2H, Ar–H), 7.88 (d, $J = 8.92$ Hz, 2H, Ar–H), ^{13}C-NMR (125 MHz, $CDCl_3$) δ (ppm): 14.17, 32.48, 55.29, 61.38, 114.13, 115.50 (d, $J =$ 21 Hz), 125.48, 128.5 (d, $J = 8.75$ Hz), 129.35, 138.04, 153.98, 158.99, 161.74, 163.65 (d, $J = 248.7$ Hz), 169.45, 171.36. Anal. calcd. for $C_{20}H_{18}FN_3O_3S$: C, 60.14; H, 4.54; N, 10.52. Found: C, 60.21; H, 4.59; N, 10.58.

Ethyl 2-(5-(4-chlorophenyl)-6-(4-methoxyphenyl)-1,2,4-triazine-3-ylthio) acetate (**8d**) Yield 65%; IR (KBr, cm^{-1}) υ_{max}: 1746 (C=O). ^{1}H-NMR (400 MHz, $CDCl_3$) δ(ppm): 1.22 (t, $J = 7.12$ Hz, 3H, $CH_2\underline{CH_3}$), 3.86 (s, 3H, OCH_3), 3.97 (s, 2H, $S\underline{CH_2}CO$), 4.25 (q, $J = 7.12$ Hz, 2H, $\underline{CH_2}CH_3$), 7.1 (d, $J = 8.96$ Hz, 2H, Ar–H), 7.35 (d, $J = 8.78$ Hz, 2H, Ar–H), 7.5 (d, $J = 8.64$ Hz, 2H, Ar–H), 8.1 (d, $J = 8.96$ Hz, 2H, Ar–H). ^{13}C-NMR (100 MHz, $CDCl_3$) δ (ppm):14.22, 33.16, 55.50, 60.90, 114.54, 127.42, 127.90, 129.26, 130.73, 132.18, 133.20, 136.68, 156.22, 164.97, 169.58, 171.27. MS, *m/z* (%): 415.0 (M^+, 5), 355.1 (23), 281.0 (22), 271.0 (17), 259.0 (19), 237.0 (35), 207.0 (49). Anal. calcd. for $C_{20}H_{18}ClN_3O_3S$: C, 57.76; H, 4.36; N, 10.10. Found: C, 57.72; H, 4.29; N, 10.12.

Ethyl 2-(5-(4-chlorophenyl)-6-(4-methoxyphenyl)-3-thioxo-1,2,4-triazin-2(3H)-yl)acetate (**8e**) Yield 10%; IR (KBr, cm^{-1}) υ_{max}: 1756 (C=O). ^{1}H-NMR (400 MHz, $CDCl_3$) δ (ppm): 1.30 (t, $J = 7.12$ Hz, 3H, $CH_2\underline{CH_3}$), 3.88 (s, 3H, OCH_3), 4.24 (q, $J = 7.16$ Hz, 2H, $\underline{CH_2}CH_3$), 4.67 (s, 2H, $N\underline{CH_2}CO$), 7.0 (d, $J = 8.96$ Hz, 2H, Ar–H), 7.32 (d, $J = 8.68$ Hz, 2H, Ar–H), 7.53 (d, $J = 8.64$ Hz, 2H, Ar–H), 8.04 (d, $J = 8.92$ Hz, 2H, Ar–H). ^{13}C-NMR (100 MHz, $CDCl_3$) δ(ppm):14.22, 55.60, 60.98, 71.35, 114.34, 127.52, 127.94, 129.06, 130.93, 132.28, 133.24, 136.58, 156.13, 164.87, 169.38, 191.40. MS, *m/z* (%): 415.0 (M^+, 1), 355.1 (5), 281.0 (14), 271.0 (9), 259.0 (13), 238.0 (45), 206.0 (47). Anal. calcd. for $C_{20}H_{18}ClN_3O_3S$: C, 57.76; H, 4.36; N, 10.10. Found: C, 57.82; H, 4.39; N, 10.22.

In vitro stability study

The stability of compound **8e** was evaluated by monitoring its UV absorbance within 2 weeks. Different concentrations of **8e** (1, 10, 25, and 50 µM) were prepared in different organic solutions (ethanol, chloroform, and DMF) and also in phosphate buffer in pH = 7.4 and changes in UV spectrum within 2 weeks at 25 °C showed subtle variations indicating its stability at room temperature.

H_2O_2-induced toxicity in PC12 cells

PC12 cells (pheochromocytoma of the rat adrenal medulla) were cultured in RPMI 1640 medium supplemented with 10 % FCS, 100 units/ml penicillin and 100 µg/ml streptomycin (All from GIBCO, Grand Island, NY, USA). After trypsinization, the cells were equally seeded into 96-well culture plates (1×10^4 cells/well). To induce neuronal differentiation the following protocol was applied. The cells were cultured in serum-free medium for 2 days, afterwards NGF (50 ng/ml, Sigma) was added until neurite outgrowth could be observed (Koh et al. 2003). For neuroprotectivity assay, initially non-toxic concentration of the final compounds on PC12 cells was determined and then differentiated PC12 cells were pretreated with different non-toxic concentrations (1–50 µM) of compounds for 3 h. Subsequently, freshly prepared H_2O_2 (final concentration 350 µM) was added to the cells and incubated for 24 h. Induction of apoptosis was recognized by DAPI staining. To determine the EC50 values of neuroprotection, different concentrations of the tested compounds were evaluated for their protective activity and the cell viability was determined. To calculate EC50 values, four different concentrations which showed cell viability in the range of 20–80% were chosen. EC50s

were calculated using GraphPad Prism 5 (GraphPad Software, San Diego, CA).

Aβ-induced toxicity in SH-SY5Y cells

β-amyloid (1–42) peptide was purchased from Sigma Aldrich. 0.1 mg peptide was dissolved in 0.02 M NaOH and diluted in PBS pH 7.4 at a concentration of 50 µM. β-amyloid (1–42) peptide was incubated at 37 °C for 7 days to induce peptide aggregation (Unsal-Tan et al. 2017; Ozadali-Sari et al. 2017).

SH-SY5Y human neuroblastoma cells were cultured in Dulbecco's modified Eagle medium (DMEM) supplemented with 10% FBS and 1% antibiotics at 37 °C in %5 CO_2. Cells were differentiated into neurons with 10 µM retinoic acid treatment for 10–15 days (Chimon et al. 2007). SH-SY5Y cells (5000 cells/well) were treated with compounds **3a–f**, **8a–e** (25 µM) for 3 h prior to β-amyloid (1–42) treatment (5 µM) and incubated for 24, 48, and 72 h. MTT reduction and LDH release assays were performed to evaluate cell viability. Annexin V/PI staining and TUNEL assay were performed to evaluate effect of compound **8e** on amyloid induced apoptosis.

Inquiry of cell viability by MTT assay

After 24, 48, and/or 72 h incubation, the medium was removed, cells were washed with PBS and 10 µl of MTT [3-(4,5-dimethylthiazolyl-2-yl)-2,5-diphenyl-tetrazolium bromide] solution (5 mg/ml, Sigma) was added to each well. After 3.5 h of incubation the medium was removed and 150 µl DMSO was added to dissolve formazan precipitates. Finally, optical density (OD) was measured at 560 nm (reference at 690 nm) using microplate reader (BioTek synergy HT) (Datki et al. 2003).

The viability (%) was calculated as follows:

$$\%\ \text{of viability} = \frac{\text{Average OD of treated wells} - \text{average OD of blank wells}}{\text{Average OD of control wells} - \text{average OD of blank wells}} \times 100$$

Lactate dehydrogenase (LDH) assay

The LDH assay is a method for viability via activity of lactate dehydrogenase (LDH) released from damaged cells. After 24, 48, and 72 h incubation, 50 µl cell culture supernatant of each well was mixed with 50 µl substrate mixture (6.6 mM NADH and 30 mM Sodium pyruvate in 0.2 M Tris·HCl buffer, pH 7.3) and incubated for 5 min at room temperature. Reaction was stopped by adding 50 µl 0.01 N HCl and absorbance was read at 340 nm. The cytotoxicity (%) was calculated as follows:

$$\%\,\text{Cytotoxicity} = \frac{\text{Compound treated LDH activity} - \text{Spontaneous LDH activity}}{\text{Maximum LDH activity} - \text{Spontaneous LDH activity}} \times 100$$

DAPI staining to evaluate induction of apoptosis

DAPI staining was performed to evaluate the effect of H_2O_2 apoptosis induction. For this purpose the differentiated PC12 cells were cultured in 96-well plate and treated with different doses of drugs as indicated above and stained with the DNA-specific fluorochrome 4′,6-diamidino-2-phenylindole dihydrochloride (DAPI, Sigma). DAPI was added to the culture medium of live cells with the final concentration of 1 µg/ml for 20 min. Due to cell membrane permeability of apoptotic cell, DAPI penetrate into the cell and makes the nucleus stained, while normal cell is not permeable sufficiently and gets lightly stained.

Annexin V/PI staining

Cells were harvested 24 or 48 h after treatment and stained using Tali™ apoptosis kit (Life Technologies) as described by the manufacterer's instructions and evaluated using the Tali™ Image-based Cytometer (Life Technologies). The annexin-V positive/PI negative cells were admitted as apoptotic, whereas the annexin V positive/PI positive cells were identified as necrotic. Dual negative stained cells were identified as viable cells (Koopman et al. 1994).

TUNEL assay

Amyloid induced apoptosis in differantiated SHSY5Y cells (±**8e** treatment) was detected and quantified by transferase-mediated dUTP nick end labeling (TUNEL) assay using Millipore ApopTag® Plus Peroxidase In situ Apoptosis Kit (S7101). Qualitative morphometric analysis was performed by light microscopy (Nikon TS 100F microscobe). Cells with nuclear staining were accepted apoptotic (TUNEL-positive) (Fried et al. 1976).

Statistical analysis

GraphPad Prism 5 Software was used to perform statistical tests. One-way analysis of variance (one-way ANOVA) followed by Dunnett test or two tailed *t*-test (where appropriate) were used to compare the significance of groups.

Results and discussion

Chemistry

The synthetic routes to the final compounds **3a–f** and **8a–e** are outlined in Schemes 1 and 2, respectively. The synthesis of symmetrical ethyl 5,6-bisaryl-1,2,4-triazine-3-ylthioacetate derivatives (**3a–f**) was started by 1,2-diketones **1a–f** in which triazine ring closure was performed by thiosemicarbazide in a mixture of water and ethanol and a few drops of hydrochloric acid under microwave irradiation (Irannejad et al. 2014, 2015). In the next step, alkylation was done at sulfur atom of thiol group by adding ethyl chloroacetate at room temperature in the presence of potassium carbonate in dimethylsulfoxide to afford compounds **3a–f**. The synthetic route for the preparation of unsymmetrical compounds **8a–e** (Scheme 2) was started by an acylation reaction of anisole with phenylacetic acid derivatives **4a–d** in the presence of trifluoroacetic anhydride and phosphoric acid. The oximation reaction in the alpha position of carbonyl group was performed by successive use of sodium methoxide and butyl-nitrite to give compounds **6a–d**. The next two steps, triazine ring closure and thiol-alkylation were performed in similar conditions as described earlier for symmetrical compounds to afford final compounds **8a–d**. In the final step, the reaction of **7a–d** with ethyl chloroacetate resulted in the formation of

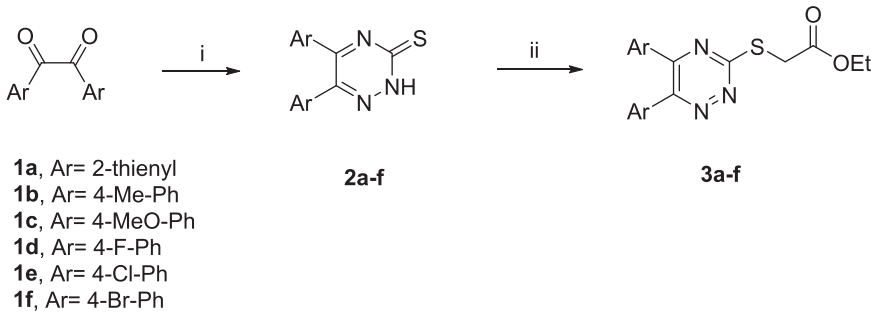

1a, Ar= 2-thienyl
1b, Ar= 4-Me-Ph
1c, Ar= 4-MeO-Ph
1d, Ar= 4-F-Ph
1e, Ar= 4-Cl-Ph
1f, Ar= 4-Br-Ph

2a-f

3a-f

Scheme 1 Reagents and conditions: (i) thiosemicarbazide, HCl, H_2O: EtOH, MW, 130 °C, 20 min. (ii) ethyl chloroacetate, K_2CO_3, DMSO, rt, 10 h

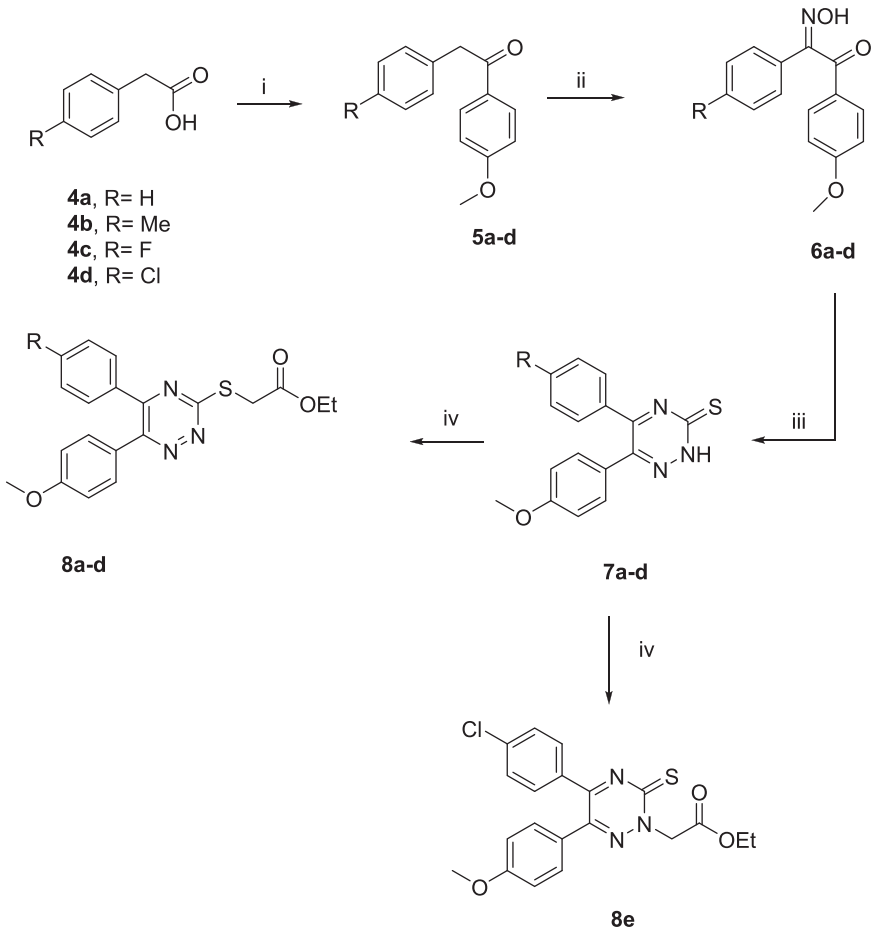

4a, R= H
4b, R= Me
4c, R= F
4d, R= Cl

5a-d

6a-d

7a-d

8a-d

8e

Scheme 2 Reagents and conditions: (i) Anisole, TFAA, H_3PO_4, rt, 5 min; (ii) MeONa, MeOH then BuONO, rt, 30 min; (iii) Thiosemicarbazide, H_2O, HCl, reflux, 4 h; (iv) ethyl chloroacetate, K_2CO_3, DMSO, rt, 10 h

S-substituted derivatives **8a–d** as major products which were purified by column chromatography. Surprisingly, in the case of 4-chloro derivative **8d**, its N-substituted regioisomer **8e** was also isolated and characterized as a minor product (yield <10%). Chemical structures of the final compounds **3a–f** and **8a–e** along with their melting point and quantitative yields for the last step are summarized in Table 1.

The FT-IR, MS, ^{1}H and ^{13}C NMR spectra were appropriately confirmed the chemical structure of final compounds **3a–f** and **8a–e** (the NMR spectra of some representative compounds are in Supplementary material). In the FT-IR spectra of these compounds, the characteristic band appearing in the range of 1724–1756 cm^{-1} confirms existence of the carbonyl group of ester moiety. In the ^{1}HNMR spectra, ethyl group of ester function shows a triplet and quartet at about 1.2 and 4.2 ppm, respectively while methylene group of acetate side chain appears at about 3.8–4.1 ppm as singlet form. Moreover, aromatic protons for the two *para*-substituted aromatic or the two thienyl rings could be easily assigned in the range of 6.8–8.0 ppm. A minor product was also isolated in the preparation of compound **8d** and its chemical structure was identified as N-substituted regioisomer **8e** by means of ^{1}H, ^{13}C, and HSQC NMR spectra. Accordingly, the chemical shift of methylene protons of compound **8e** was seen to be desheilded to 4.6 ppm. Inspection of HSQC spectrum of compound **8e** reveals chemical shift of the side chain methylene carbon of **8e** to be 71.35 ppm, 40 units more than the same carbon atom for other S-substituted compounds (Fig. 3, Table 2).

Further confirmation of this possible structure is based on the unexpected chemical shift of C3-carbon atom of triazine ring at 191.40 ppm that is 20 units of ppm more than the same atom on the other S-substituted final compounds and highly favors the possible ex35istence of a thione group on the C3-carbon atom of triazine ring of regioisomer **8e**. Therefore, these observations have truly confirmed the linkage of methylene side chain to the nitrogen atom of triazine ring. Occurrence of N- over S-alkylation on 1,2,4-triazine-3(2H)-thione ring system has been reported in a previous study but with no detail structural information and discussion about synthesized compounds (Mullick et al. 2009). In the case of **8a–c** and under the current experimental protocol, some traces of by-products were observed by TLC but not as much that could be isolated and characterized. Probably, some change in experimental procedure would be inevitable to obtain N-alkylated regioisomers of **8a–c** and also to increase the production yield of **8e**.

Neuroprotective activity against H_2O_2-induced toxicity in PC12 cells

β-amyloid induced neurotoxicity involves several components as increased oxidative stress, mitochondrial dysfunction, DNA damage and elevated apoptotic events. H_2O_2 is documented to induce apoptosis and contribute to β-amyloid induced neuronal death (Behl et al. 1994; Tamagno et al. 2003; Saito et al. 2001).

The ability of compounds to antagonize the oxidative insult was evaluated in H_2O_2-treated PC12 cells by MTT assay. The EC_{50} values (concentration of compounds in which 50% of cells are viable in the presence of H_2O_2) were determined for compounds as shown in Table 3. All compounds showed significant neuroprotective activity against H_2O_2-induced toxicity with EC_{50} values ranging from 14 to 30 μM. Compounds 8e and 3e were found to be the most neuroprotective agents with EC_{50} values of 14.44 and 17.86 μM, respectively. Quercetin as a well-known neuroprotective agent was used as a reference drug for comparison and could protect PC12 cells against H_2O_2 with EC_{50} of 8 μM.

There is marginal difference between EC_{50} values of unsymmetrical compounds **8a–d** (20–23 μM) but higher variations in symmetrical ones (17–23 μM) which could be mostly due to the presence of two new atoms in each compound structure in symmetrical ones.

In the symmetrical compounds, **3e** with chlorine-substitution on both phenyl rings was shown to be the most potent one in H_2O_2-induced toxicity assay on PC12 cells similar to unsymmetrical compounds in which the chlorine-substituted derivatives **8d** and its regioisomer **8e** were the best ones in this group (Table 3).

Morphological assessment was used to indicate the apoptotic state of cells treated with H_2O_2 or neuroprotective agents. As illustrated in Fig. 4, normal cells differentiate in from of neurite outgrowth while apoptotic cells have DNA condensation and fragmented parts identified by blue stains after DAPI staining. The neuroprotective effect of compound **8e** against H_2O_2-induced apoptosis in PC12 cells was investigated by DAPI staining. Pretreatment with compound **8e** (20 μM) could substantially reduce apoptotic markers as DNA condensation and fragmentation compared to H_2O_2 treated group (Fig. 5).

Neuroprotective activity against β-amyloid induced toxicity in SH-SY5Y cells

Amyloid peptide (1–42) accumulation has been proposed to have significant role in the pathogenesis of AD and incidence of neurotoxicity (Novitskaya et al. 2006). SH-SY5Y cells are neuroblastoma cells that differentiate into neuronal cells by retinoic acid treatment (Dwane et al. 2013).

To evaluate the neuroprotective effects of compounds against β-amyloid (1–42) peptide induced cytotoxicity, SH-SY5Y cells were pretreated with compounds **3a–f** and **8a–e** (25 μM) and cell viability was determined by MTT assay. The data is expressed in Fig. 6 as percent of cell viability compared to normal cells (100% viability) at 24 h.

Table 1 Chemical structures and physicochemical properties of synthesized compounds **3a–f** and **8a–e**

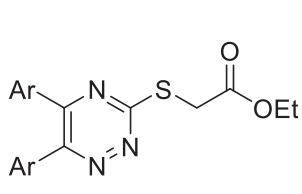

3a-f

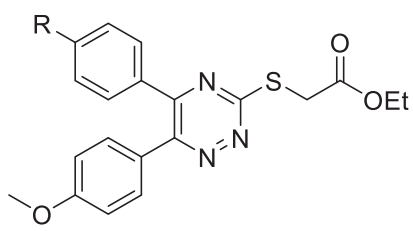

8a-d

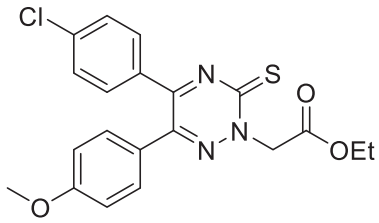

8e

Entry	Compound	Ar	R	MW	Formula	mp (°C)	Yield (%)[a]
1	**3a**	2-thienyl	–	363.47	$C_{15}H_{13}N_3O_2S_3$	185–186	86
2	**3b**	4-Me–C_6H_5	–	379.48	$C_{21}H_{21}N_3O_2S$	164–165	80
3	**3c**	4-MeO–C_6H_5	–	411.47	$C_{21}H_{21}N_3O_4S$	172–173	75
4	**3d**	4-F–C_6H_5	–	387.40	$C_{19}H_{15}F_2N_3O_2S$	158–159	51
5	**3e**	4-Cl–C_6H_5	–	420.31	$C_{19}H_{15}Cl_2N_3O_2S$	187–188	69
6	**3f**	4-Br–C_6H_5	–	509.22	$C_{19}H_{15}Br_2N_3O_2S$	170–171	76
7	**8a**	–	H	381.45	$C_{20}H_{19}N_3O_3S$	93–94	61
8	**8b**	–	CH_3	395.47	$C_{21}H_{21}N_3O_3S$	111–112	60
9	**8c**	–	F	399.44	$C_{20}H_{18}FN_3O_3S$	122–123	53
10	**8d**	–	Cl	415.89	$C_{20}H_{18}ClN_3O_3S$	116–117	65
11	**8e**	–	–	415.89	$C_{20}H_{18}ClN_3O_3S$	126–127	<10

[a] Yields for last step reaction

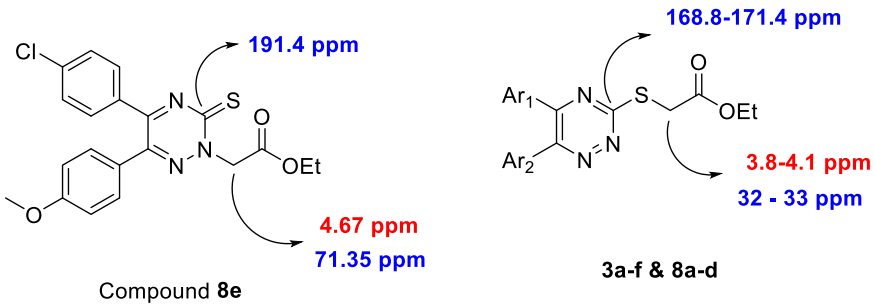

Fig. 3 ^{1}H and ^{13}CNMR Chemical shifts of the methylene group of acetate side chain and also C3 carbon atom of triazine ring in compounds **3a–f** and **8a–d** compared to the regioisomer **8e**. ^{1}HNMR chemical shifts are in *red* and ^{13}CNMR ones represented in *blue*(color figure online)

Table 2 ^{1}H, ^{13}C chemical shift data of compound **8e** provided by HSQC spectrum

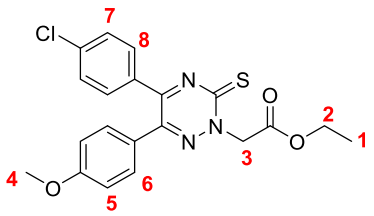

Atom no.	^{13}C (δ, ppm)	^{1}H (δ, ppm), Mult.
1	14.22	1.3, t
2	60.98	4.24, q
3	71.35	4.67, s
4	55.60	3.88, s
5	114.34	7.0, d
6	132.28	8.04, d
7	129.06	7.32, d
8	127.94	7.53, d

Table 3 Neuroprotective activity of the target compounds on H_2O_2-induced toxicity on PC12 cells

Compounds	Neuroprotective activity (EC50 ± SEM, μM)
3a	21.13 ± 1.05
3b	23.32 ± 1.89
3c	19.7 ± 2.41
3d	30.04 ± 2.78
3e	17.86 ± 2.24
3f	19.56 ± 1.2
8a	23.13 ± 2.56
8b	22.74 ± 3.69
8c	21.20 ± 1.53
8d	20.70 ± 1.23
8e	14.44 ± 0.85
Quercetin	8.18 ± 1.45

β-amyloid reduced cell viability to 51% in the absence of any neuroprotective agent compared to the normal cell (100%). In general, all compounds could increase cell viability compared to β-amyloid treated group with the exception of **3c, 3e**,and **8c**. Interestingly, the most effective compound was again found to be **8e**; pretreatment at 25 μM for 3 h increased significantly cell viability to 65% ($P < 0.01$) compared to β-amyloid treated cells (51%).

However, results on β-amyloid induced toxicity in SH-SY5Y cells showed controversy especially in symmetrical compounds in which chlorine-substituted derivative **3e** was the weakest but **3f** with bromine substituent owns the highest potency in this group. This incomparable result among symmetrical compounds may be attributed to the kind of cell used in this study. In the unsymmetrical ones there is a relevant order of variation in potency so that electron-withdrawing substituents like fluoro and chloro derivatives have more potency than compounds **8a** and **8b**. Similarly to the results obtained in H_2O_2-induced toxicity on PC12 cells, the best compound was again found to be regioisomer **8e**. Therefore, **8e** was the most potent compound in both studies.

Neuroprotective effect of compound **8e** was further studied in detail by MTT and LDH assays at 24–48 h and compared to Quercetin (25 μM). Mitochondrial activity reduction was significantly attenuated 24% (after 24 and 48 h of treatment) compared to amyloid treated cells and 8–12% compared to Quercetin-pretreated cells at 24 and 48 h, respectively. This shows that the neuroprotective activity of compound **8e** is higher than Quercetin at the same concentration and in the presence of β-amyloid. LDH release was not changed at any time points, pointing anti-apoptotic effect of compound **8e** (Fig. 7). LDH assay is an experiment to show necrotic cell death. A key signature for necrotic cells is the permeabilization of the plasma membrane and release of LDH enzyme. On the contrary, in apoptotic death mechanisms cell membrane is mostly intact and any change in LDH release is observed. Figure 7 shows that β-amyloid 1–42 treatment induces apoptosis rather than necrosis.

We further examined the anti-apoptotic role of the most potent neuroprotective compound **8e** against amyloid induced cytotoxicity via Annexin V/PI staining and TUNEL assay.

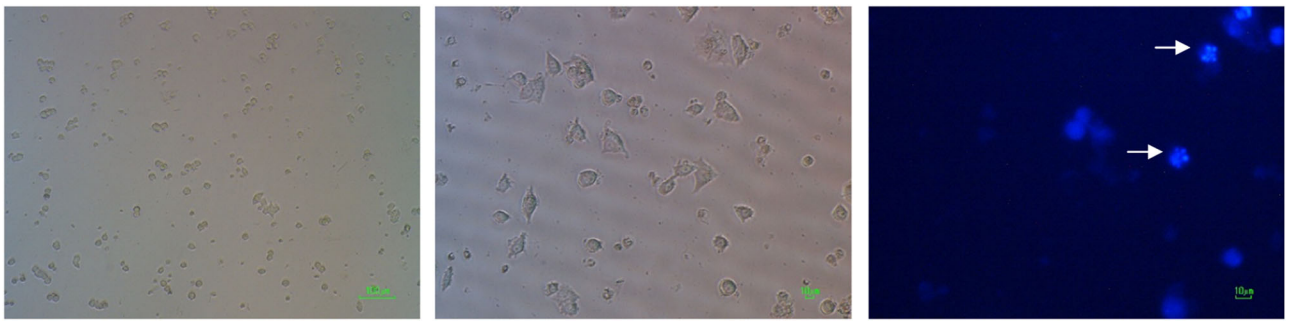

Fig. 4 *Left* undifferentiated PC12 cells; *Middle* Differentiated PC12 cells showing neurite outgrowth; *Right* Apoptotic cells stained with DAPI (intense *blue*) in H_2O_2-treated group, DNA condensation and fragmentation is obvious in apoptotic cells (marked by *arrows*) (color figure online)

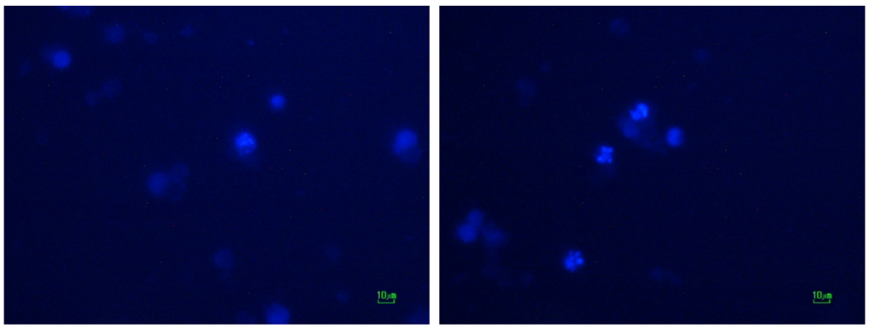

Fig. 5 Morphological assessment of cells using DAPI staining. Differentiated PC12 cells were treated with **8e** (20 μM) followed by exposure to H_2O_2. *Left* compound **8e** treated group in the presence of H_2O_2. *Right* H_2O_2-treated group, DNA condensation and fragmentation is obvious in apoptotic cells

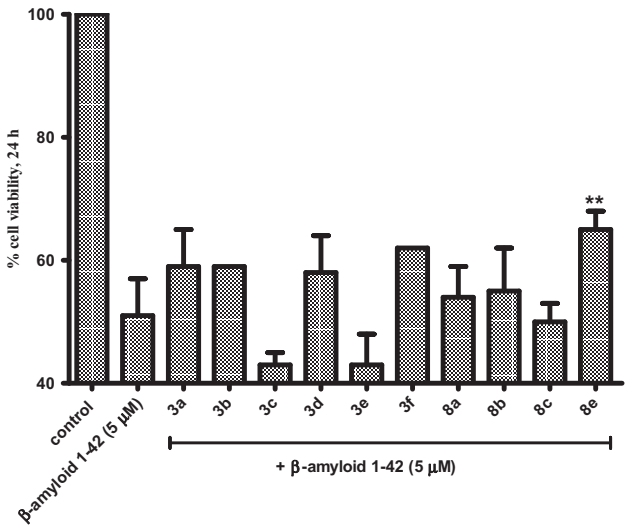

Fig. 6 Effects of pretreatment with test compounds on Aβ-induced cell death at 24 h. Values are means ±SEM ($n = 3$). (**$P < 0.01$, compared to amyloid treated group)

Cytometric analysis with Annexin V/Propidium iodide staining

Studies of cellular apoptosis have been significantly impacted since the introduction of cytometry-based methods. Phosphatidylserine (PS) residues is normally absent on the plasma membrane but its appearance on cell surface is an early sign of apoptosis, and can be used to detect and measure apoptosis. During apoptosis, PS is transferred from the inner or cytoplasmic face of the plasma membrane to the cell surface. Annexin V has a strong, Ca^{2+}-dependent affinity for PS and therefore can be used as a probe for detecting apoptosis.

Propidium iodide (PI) in combination with Annexin V is widely used to determine if cells are viable, apoptotic, or necrotic through differences in plasma membrane integrity and permeability. The Annexin V/PI protocol is a commonly used method for studying apoptotic cells. The ability of PI to enter a cell is dependent upon the integrity of the membrane; PI does not stain live or early apoptotic cells due to the presence of an intact plasma membrane. In late apoptotic and necrotic cells, disruption of the integrity of plasma and nuclear membranes allows PI to pass through the membranes, intercalate into nucleic acids, and display red fluorescence.

Apoptosis is a cellular mechanism for programmed cell death. Early apoptotic events are characterized by pyknotic nuclei and membrane blebbing while late apoptosis may be determined by disintegrated nucleus membrane (Yakovlev and Faden 2004).

To evaluate the effect of compound **8e** on β-amyloid (1–42) peptide induced apoptosis (5 μM) for 24 and 48 h, differentiated SH-SY5Y cells with or without **8e** pretreatment (25 μM for 3 h) were evaluated by Tali apoptosis kit and the results are presented in Fig. 8. Interestingly, compound **8e** significantly increased ($P < 0.005$) cell viability

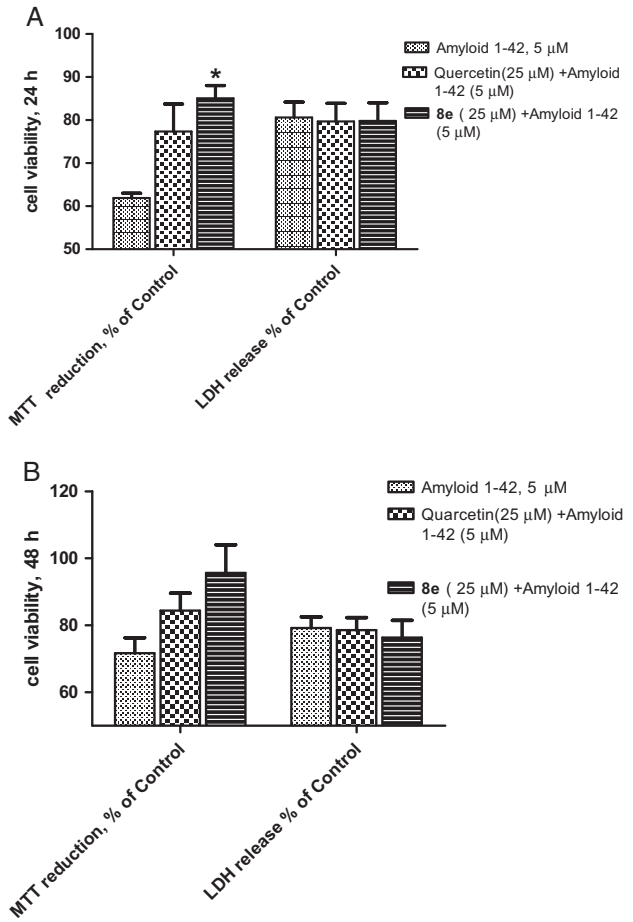

Fig. 7 Protective effects of **8e** on β-amyloid induced cell death. Mitochondrial activity reduction and LDH release. **a** 24 h **b** 48 h. Values are means ±SEM ($n = 3$). (*$P < 0.05$, compared to amyloid treated group)

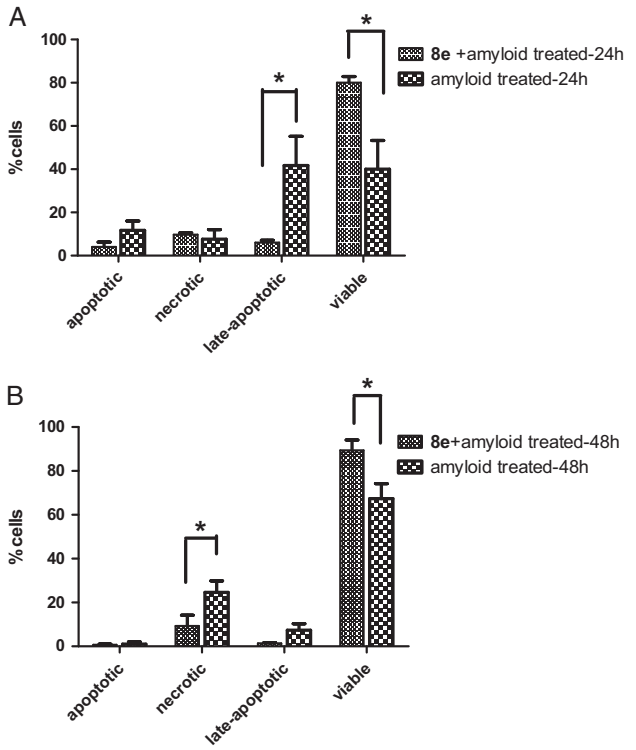

Fig. 8 Evaluation of neuroprotective effect of **8e** (25 μM) pretreatment for 3 h on β-amyloid peptide 1–42 induced apoptosis (5 μM) for 24 h (**a**) and 48 h (**b**); Values are means ±SEM ($n = 3$). (*, $p < 0.005$ vs. only amyloid treated by two tailed *t*-test)

from 40 to 80% and 67 to 89% at 24 and 48 h compared to β-amyloid treated cells, respectively.

Moreover, compound **8e** attenuated late-apoptosis from 42 to 6% ($P < 0.005$) and 7 to 1% at 24 and 48 h respectively compared to amyloid treated cells. Similarly, apoptosis was reduced from 12 to 4% at 24 h, although no substantial changes were evident in apoptotic percentage of **8e** treated cells at 48 h. Decrease in late apoptosis and cell death at 48 h would be late to observe amyloid induced apoptosis. These findings were compatible with recent reports demonstrating β-amyloid induced neuronal apoptosis even at 6 h (Zhu et al. 2014).

Necrosis is an unprogrammed type of cell death due to the loss of membrane integrity which is followed by cell lysis. Necrosis is usually induced in neuronal cells with exposure to toxins and reactive oxygen species (Ziegler and Groscurth 2004). With the release of the cellular components and increased reactive species, acute inflammation usually occurs in response to necrotic cell death. Although a statistically negligible increase in necrotic cells was determined at 24 h, **8e** pretreatment significantly decreased ($P < 0.005$) necrosis from 25 to 9% at 48 h.

Morphological evaluation with TUNEL assay

Terminal deoxynucleotidyl transferase (TdT) dUTP Nick-End Labeling (TUNEL) assay has been widely used to detect apoptotic cells that undergo extensive DNA degradation during the late stages of apoptosis. The assay relies on the presence of nicks in the DNA which can be identified by terminal deoxynucleotidyl transferase (TdT), an enzyme that catalyzes the addition of dUTPs that are secondarily labeled with a marker to the blunt ends of double-stranded DNA breaks. It may also label cells that have suffered severe DNA damage.

Tunel assay was carried out to assess the morphological changes of cell death in vitro. As shown in Fig. 9, β-amyloid (1–42) treatment induced apoptosis at 24 h (Fig. 9a) that is followed by necrosis at 48 h (Fig. 9c) in which apoptotic cells are characterized by condensed chromatin, disintegration of cell membrane and accumulated cells.

Pretreatment with **8e** for 3 h remarkably reduced cell death after 24 h (Fig. 9b) and late-apoptosis after 48 h (Fig. 9d) respectively. As depicted in Fig. 9b, cells have normal appearance in the presence of compound 8e at 24 h but late-

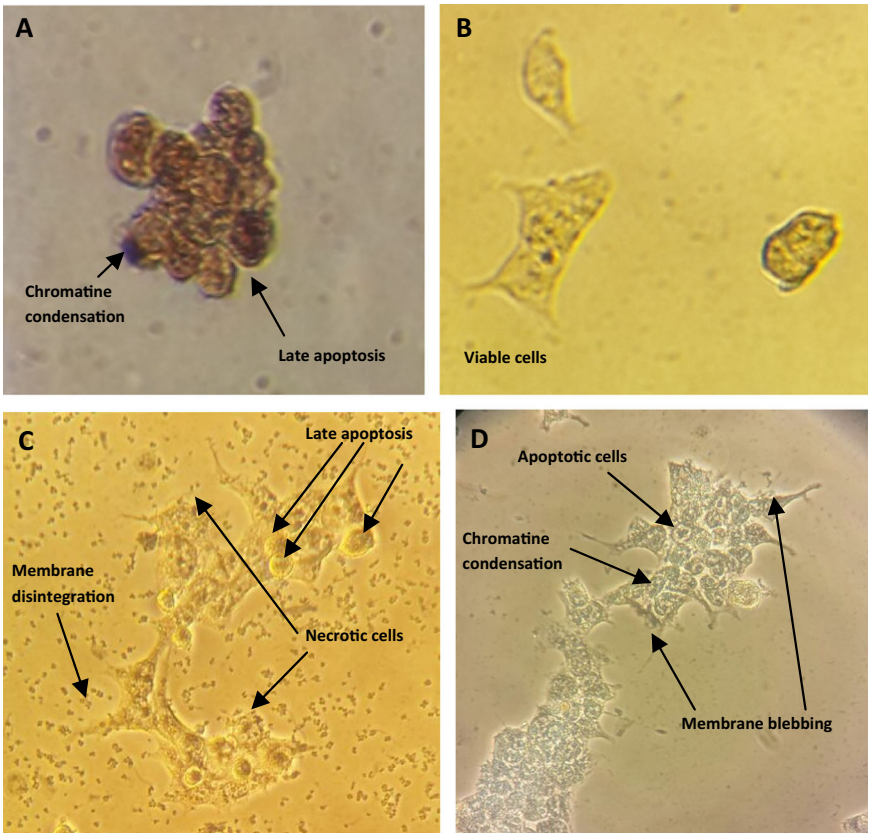

Fig. 9 TUNEL staining of differentiated SH-SY5Y cells after 24 h exposure to **a** β-amyloid peptide 1–42 (5 μM) **b** pretreatment with **8e** (25 μM) for 3 h + β-amyloid peptide 1–42 (5 μM). After 48 h exposure to **c** β-amyloid peptide 1–42 (5 μM) **d** pretreatment with **8e** (25 μM) for 3 h + β-amyloid peptide 1–42 (5 μM). Necrotic cells showed membrane disintegration and diffused chromatin. Apoptotic cells showed membrane blebbing and chromatine condensation

apoptosis is obvious at 48 h due to the beta-amyloid induced neurotoxicity.

Based on our previous research in the past few years, 5,6-diaryl-1,2,4-triazine compounds have shown to be dual Cyclooxygenase and β-amyloid aggregation inhibitors and hence explains the mechanism behind ability of these compounds to reduce cell toxicity probably through dual mechanism of action (Dadashpour et al. 2015).

Prediction of solubility and lipophilicity

Lipophilicity and solubility are two major issues which have to be evaluated especially for CNS active drug candidates. The predicted values of these two physicochemical parameters for compounds **3a–f** and **8a–e** are calculated and represented in Table 4. As shown, most of the logP values are less than 5 except compounds **3e** and **3f**. Therefore, according to the Lipinski's rule of 5, most of compounds would have good oral bioavailability and permeability across biologic membranes. However compounds **3a–f** and **8a–e** have an ester group and therefore could be considered as *prodrugs*, which helps them to permeate easily through membranes. On the other hand, one might think of low solubility of compounds **3a–f** and **8a–e** due to their high lipophilic character. Indeed, after passage into membranes and being exposed to body fluids, hydrolyzation of ester function and conversion to acidic group is inevitable in vivo in the presence of various and abundant amounts of esterase enzymes in the body. Actually, free acidic form of compounds would have acceptable solubility as predicted in Table 4. Since more than 80% of drugs on the market have an estimated logS value greater than −4, shows that our synthesized compounds have admissible solubility. Calculated logD of compounds in the range of 0.1–2.0 truly confirms a good balance between lipophilicity and

Table 4 Predicted logP of parent compounds, logS and logD (pH 7.4) values of hydrolyzed compounds (acidic form)

Compd	logP	logS (acidic form)	logD (acidic form)
3a	3.7	−1.6	0.4
3b	5.1	−3.1	1.6
3c	3.8	−1.9	0.1
3d	4.4	−2.3	0.6
3e	5.3	−3.3	1.6
3f	5.6	−3.9	2.0
8a	3.9	−2.0	0.4
8b	4.5	−2.5	0.9
8c	4.1	−2.0	0.4
8d	4.5	−2.6	0.9
8e	4.4	−2.3	0.6

Calculated by ChemAxon

solubility and capability of compounds to pass through blood-brain barrier according to the reported literature (van de Waterbeemd et al. 1998).

Conclusion

In order to find new agents with beneficial effect against AD, we introduced some 5,6-diaryl-1,2,4-triazine derivatives and evaluated them against H_2O_2- and β-amyliod induced toxicity in PC12 and SH-SY5Y cell lines respectively. Interestingly, all compounds showed remarkable neuroprotective effect in PC12 cell line. Particularly, the N-substituted regioisomer **8e** was the most potent compound with EC_{50} of 14 μM in H_2O_2 induced toxicity assay and was also the most potent one against toxic effect of β-amyloid peptide. Further morphological evaluation revealed the ability of this compound to prevent apoptosis and DNA fragmentation in treated cells. Eventually, compound **8e** could be considered as a novel neuroprotective agent in developing anti-Alzheimer's leading drugs and further studies would be enlightening the underlying mechanisms involved in the neuroprotective activity of regioisomer **8e** in future. Furthermore, it demands more effort to synthesize new and various substituted derivatives of N-alkylated regioisomer **8e** and evaluate their neuroprotective ability in the future.

Acknowledgements This research was supported by grant from the Research Council of Mazandaran University of Medical Sciences. This study is related to the Pharm.D thesis of K. Safari Yanghagh and M.A. Roknipour.

Compliance with ethical standards

Conflict of interest The authors declare that they have no competing interests.

References

Ansari N, Khodagholi F, Ramin M, Amini M, Irannejad H, Dargahi L, Amirabad AD (2010) Inhibition of LPS-induced apoptosis in differentiated-PC12 cells by new triazine derivatives through NF-κB-mediated suppression of COX-2. Neurochem Int 57:958–968

Behl C, Davis JB, Lesley R, Schubert D (1994) Hydrogen peroxide mediates amyloid beta protein toxicity. Cell 77:817–827

Butterfield DA (2002) Amyloid beta-peptide (1-42)-induced oxidative stress and neurotoxicity: implications for neurodegeneration in Alzheimer's disease brain. A review. Free Radic Res 36:1307–1313

Cheng B, Lin Y, Kuang M, Fang S, Gu Q, Xu J, Wang L (2015) Synthesis and anti-neuroinflammatory activity of lactone benzoyl hydrazine and 2-nitro-1-phenyl-1h-indole derivatives as p38α MAPK inhibitors. Chem Biol Drug Des 86:1121–1130

Chimon S, Shaibat MA, Jones CR, Calero DC, Aizezi B, Ishii Y (2007) Evidence of fibril-like β-sheet structures in a neurotoxic amyloid intermediate of Alzheimer's β-amyloid. Nat Struct Mol Biol 14:1157–1164

Dadashpour S, Tuylu Kucukkilinc T, Unsal Tan O, Ozadali K, Irannejad H, Emami S (2015) Design, synthesis and in vitro study of 5,6-diaryl-1,2,4-triazine-3-ylthioacetate derivatives as COX-2 and beta-amyloid aggregation inhibitors. Arch Pharm 348:179–187

Datki Z, Juhasz A, Galfi M, Soos K, Papp R, Zadori D, Penke B (2003) Method for measuring neurotoxicity of aggregating polypeptides with the MTT assay on differentiated neuroblastoma cells. Brain Res Bull 62:223–229

Dwane S, Durack E, Kiely PA (2013) Optimizing parameters for the differentiation of SH-SY5Y cells to study cell adhesion and cell migration. BMC Res Notes 6:366

Findeis MA (2007) The role of amyloid beta peptide 42 in Alzheimer's disease. Pharmacol Ther 116:266–286

Fried J, Perez AG, Clarkson BD (1976) Flow cytofluorometric analysis of cell cycle distributions using propidium iodide. Properties of the method and mathematical analysis of the data. J Cell Biol 71:172–181

Geng V, Li M, Ren JS, Wang EB, Qu XG (2011) Polyoxometalates as inhibitors of the aggregation of amyloid β peptides associated with Alzheimer's disease. Angew Chem Int Ed 50:4184–4188

Ghosh AK, Osswald HL (2014) BACE1 (β-secretase) inhibitors for the treatment of Alzheimer's disease. Chem Sec Rev 43:6765–6813

Heneka M, O'Banion MK, Terwel D, Kummer M (2010) Neuroinflammatory processes in Alzheimer's disease. J Neural Transm 117:919–947

Irannejad H, Amini M, Khodagholi F, Ansari N, Khoramian Tusi S, Sharifzadeh M, Shafiee A (2010) Synthesis and in vitro evaluation of novel 1,2,4-triazine derivatives as neuroprotective agents. Bioorg Med Chem 18:4224–4230

Irannejad H, Naderi N, Emami S, Foroumadi A, Qobadi Ghadikolaei R, Zafari T, Mazar-Atabaki A, Dadashpour S (2014) Microwave assisted synthesis and anticonvulsant activity of 5,6-bisaryl-1,2,4-triazine-3-thiol derivatives. Med Chem Res 23:2503–2514

Irannejad H, Nadri H, Naderi N, Rezaeian SN, Zafari N, Foroumadi A, Amini M, Khoobi M (2015) Anticonvulsant activity of 1,2,4-triazine derivatives with pyridyl side chain: synthesis, biological, and computational study. Med Chem Res 24:2505–2513

Khodagholi F, Ansari N, Amini M, Khoramian Tusi S (2012a) Involvement of molecular chaperones and the transcription factor Nrf2 in neuroprotection mediated by para-substituted-4,5-diaryl-3-thiomethyl-1,2,4-triazines. Cell Stress and Chaperones 17:409–422

Khodagholi F, Khoramian Tusi S, Zeighamy Alamdary S, Amini M, Ansari N (2012b) 3-Thiomethyl-5,6-(dimethoxyphenyl)-1,2,4-triazine improves neurite outgrowth and modulates MAPK phosphorylation and HSPs expression in H2O2-exposed PC12 cells. Toxicol in Vitro 26:907–914

Khoramian Tusi S, Ansari N, Amini M, Dehghani Amirabad A, Shafiee A, Khodagholi F (2010) Attenuation of NF-kappaB and activation of Nrf2 signaling by 1,2,4-triazine derivatives, protects neuron-like PC12 cells against apoptosis. Apoptosis 15:738–751

Koh SH, Kim SH, Kwon H, Park Y, Kim KS, Song CW, Kim J, Kim MH, Yu HJ, Henkel JS, Jung HK (2003) Epigallocatechin gallate protects nerve growth factor differentiated PC12 cells from oxidative-radical-stress-induced apoptosis through its effect on phosphoinositide 3-kinase/Akt and glycogen synthase kinase-3. Brain Res Mol Brain Res 118:72–81

Koopman G, Reutelinqsperger CP, Kuijten GA, Keehnen RM, Pals ST, van Oers MH (1994) Annexin V for flow cytometric detection of phosphatidylserine expression on B cells undergoing apoptosis. Blood 84:1415–1420

Manev H, Chen H, Dzitoyeva S, Manev R (2011) Cyclooxygenases and 5-lipoxygenase in Alzheimer's disease. Prog Neuropsychopharmacol Biol Psychiatry 35:315–319

Mullick P, Khan SA, Begum T, Verma S, Kaushik D, Alam O (2009) Synthesis of 1,2,4-triazine derivatives as potential anti-anxiety and anti-inflammatory agents. Acta Pol Pharm 66:379–385

Novitskaya V, Bocharova O, Bronstein VI, Baskakov IV (2006) Amyloid fibrils of mammalian prion protein are highly toxic to cultured cells and primary neurons. J Biol Chem 281:13828–13836

Nunan J, Small DH (2000) Regulation of APP cleavage by alpha-, beta- and gamma-secretases. FEBS Lett 483:6–10

Ozadali-Sari K, Tüylü Küçükkılınç T, Ayazgok B, Balkan A, Unsal-Tan O (2017) Novel multi-targeted agents for Alzheimer's disease: Synthesis, biological evaluation, and molecular modeling of novel 2-[4-(4-substitutedpiperazin-1-yl)phenyl]benzimidazoles. Bioorg Chem 72:208–214

Pimplikar SW (2009) Reassessing the amyloid cascade hypothesis of Alzheimer's disease. Int J Biochem Cell Biol 41:1261–1268

Raina P, Santaguida P, Ismaila A, Patterson C, Cowan D, Levine M, Booker L, Oremus M (2008) Effectiveness of cholinesterase inhibitors and memantine for treating dementia: evidence review for a clinical practice guideline. Ann Intern Med 148:379–397

Saito T, Kijima H, Kiuchi Y, Isobe Y, Fukushima K (2001) beta-amyloid induces caspase-dependent early neurotoxic change in PC12 cells: correlation with H2O2 neurotoxicity. Neurosci Lett 305:61–64

Shaykhalishahi H, Taghizadeh M, Yazdanparast R, Chang YT (2010) Anti-amyloidogenic effect of AA3E2 attenuates beta-amyloid induced toxicity in SK-N-MC cells. Chem Biol Interact 186:16–23

Sinha A, Tamboli RS, Seth B, Kanhed AM, Tiwari SK, Agarwal S, Nair S, Giridhar R, Chaturvedi RK, Yadav MR (2015) Neuroprotective role of novel triazine derivatives by activating Wnt/β catenin signaling pathway in rodent models of alzheimer's disease. Mol Neurobiol 52:638–652

van de Waterbeemd H, Camenisch G, Folkers G, Chretien JR, Raevsky OA (1998) Estimation of blood-brain barrier crossing of drugs using molecular size and shape, and H-bonding descriptors. J Drug Target 6:151–165

Veloso AJ, Dhar D, Chow AM, Zhang B, Tang DWF, Ganesh HVS, Mikhaylichenko S, Brown IR, Kerman K (2013) sym-Triazines for directed multitarget modulation of cholinesterases and amyloid-β in Alzheimer's disease. ACS Chem Neurosci 4:339–349

Tamagno E, Robino G, Obbili A, Bardini P, Aragno M, Parola M, Danni O (2003) H2O2 and 4-hydroxynonenal mediate amyloid beta-induced neuronal apoptosis by activating JNKs and p38MAPK. Exp Neurol 180:144–155

Unsal-Tan O, Ozadali-Sari K, Ayazgok B, Küçükkılınç TT, Balkan A (2017) Novel 2-Arylbenzimidazole derivatives as multi-targeting agents to treat Alzheimer's disease. Med Chem Res 26:1506–1515

Yakovlev AG, Faden AI (2004) Mechanisms of neural cell death: implications for development of neuroprotective treatment strategies. NeuroRx 1:5–16

Zhu X, Wang S, Yu L, Yang H, Tan R, Yin K, Jin J, Zhao H, Guan D, Xu Y (2014) TL-2 attenuates β-amyloid induced neuronal apoptosis through the AKT/GSK-3β/β-catenin pathway. Int J Neuropsychopharmacol 17:1511–1519

Ziegler U, Groscurth P (2004) Morphological features of cell death. News Physiol Sci 19:124–128